Motor-dependent microtubule disassembly driven by tubulin tyrosination

Leticia Peris[1], Michael Wagenbach[2], Laurence Lafanechère[3], Jacques Brocard[1], Ayana T. Moore[2], Frank Kozielski[4], Didier Job[1], Linda Wordeman[2] and Annie Andrieux[1]

[1]INSERM U836, Grenoble Institute of Neurosciences; CEA, DSV, iRTSV/GPC; University Joseph Fourier, BP170, 38042 Grenoble Cedex 9, France

[2]Department of Physiology and Biophysics, University of Washington, Seattle, WA 98195

[3]CNRS, UMR 5168 ; CEA, DSV, iRTSV/CMBA, 17 rue des Martyrs, Grenoble 38054

[4]The Beatson Institute for Cancer Research, Garscube Estate, Road, Bearsden, Glasgow G61 1BD

Correspondence to Leticia Peris (Leticia.peris@ujf-grenoble.fr) or Annie Andrieux (annie.andrieux@ujf-grenoble.fr)

Revised version 2: 200902142R, May 12th, 2009

Number of characters: 20.122

ABSTRACT

In cells, stable microtubules are covalently modified by a carboxy-peptidase which removes the C-terminal tyrosine residue of α-tubulin. The significance of this selective detyrosination of microtubules is not understood. Here, we report that tubulin detyrosination in fibroblasts inhibits microtubule disassembly. This inhibition is relieved by overexpression of the depolymerizing motor MCAK. Conversely, suppression of MCAK expression prevents disassembly of normal tyrosinated microtubules in fibroblasts. Detyrosination of microtubules suppresses the activity of MCAK *in vitro*, apparently due to a decreased affinity of the ADP-Pi and ADP bound forms of MCAK for the microtubule lattice. Detyrosination also impairs microtubule disassembly in neurons and inhibits the activity of the neuronal depolymerizing motor KIF2A *in vitro*. These results indicate that microtubule depolymerizing motors are directly inhibited by detyrosination of tubulin, resulting in stabilization of cellular microtubules. Detyrosination of transiently stabilized microtubules may give rise to persistent subpopulations of disassembly-resistant polymers to sustain sub-cellular cytoskeletal differentiation.

INTRODUCTION

Tubulin is subject to post translational modifications which principally affect the C-terminus of its α-subunit. In one of these modifications, the C-terminal tyrosine residue of α-tubulin, is cyclically removed from the peptide chain by a carboxypeptidase and then subsequently re-ligated to the chain by tubulin tyrosine ligase (TTL) (Hammond et al., 2008). This cycle generates pools of tyrosinated and detyrosinated microtubules in cells. As a rule, dynamic microtubules are tyrosinated, whereas stable polymers are detyrosinated (Schulze et al., 1987). Detyrosination *per se* does not stabilize microtubules (Khawaja et al., 1988). However, microtubule stabilization in cells induces microtubule detyrosination which is hence considered as a consequence, not a cause, of microtubule stabilization (Webster et al., 1987).

In recent years, important functions of tubulin tyrosination have been discovered. Thus, TTL loss and resulting tubulin detyrosination confers selective advantage to cancer cells during tumour growth (Mialhe et al., 2001). TTL suppression in mice, which induces massive tubulin detyrosination, leads to lethal disorganization of neuronal circuits (Erck et al., 2005). Cells derived from TTL deficient (TTL KO) mice display morphogenetic and polarity anomalies (Peris et al., 2006). Tyrosination has turned out to be crucial for tubulin interaction with CAP-Gly + end tracking proteins (Badin-Larcon et al., 2004; Bieling et al., 2008; Peris et al., 2006; Steinmetz and Akhmanova, 2008) suggesting that the phenotypes observed following TTL suppression may arise from mislocalization of CAP-Gly proteins at detyrosinated microtubule + ends. However, a mechanistic explanation for the long-recognized correlation between microtubule stability and tubulin tyrosination remains elusive. This prompted us to re-examine the relationship of tubulin tyrosination with microtubule dynamics, using TTL KO cells in which microtubules are extensively detyrosinated. We found that the tyrosination status of the microtubule had a profound effect on the microtubule-depolymerization activity of kinesin-13 family members.

RESULTS AND DISCUSSION

We initially observed decreased microtubule sensitivity to the depolymerizing drug nocodazole in TTL KO MEFs compared to WT (Fig. 1A), suggesting that microtubules are stabilized in TTL KO MEFs. We have previously shown that the interaction of microtubules with stabilizing factors such as structural MAPs or + end binding proteins is either unaffected or inhibited by tubulin detyrosination (Peris et al., 2006; Saoudi et al., 1995). Therefore, we hypothesized that in TTL KO cells, detyrosinated microtubules might be poor substrate for microtubule destabilizing factors, such as the kinesin-13 protein MCAK (mitotic centromere-associated kinesin) which is an important depolymerizing motor in cycling cells (Hedrick et al., 2008; Manning et al., 2007; Mennella et al., 2005; Newton et al., 2004; Ohi et al., 2007). Thereby, MCAK overexpression should rescue the loss of dynamic microtubules in TTL KO cells. Conversely, suppression of MCAK expression should prevent disassembly of normal tyrosinated microtubules in fibroblasts To test these possibilities, individual microtubule dynamics were monitored in WT or TTL KO MEFs. Cells were either untreated, transfected with MCAK cDNA, or with MCAK siRNAs (Supplementary Information, Fig. S1D shows MCAK depletion by siRNAs). Microtubule behavior was scored close to the membrane in lamellipodial extensions.

In WT MEFs, most microtubules depolymerized upon contact with the membrane (Fig. 1B). In contrast, many microtubules continued to grow tangential to the leading edge after touching the membrane in TTL KO MEFs (Fig.1B and Supplementary videos 1-2). The time spent by microtubules close to the membrane (persistence time) was markedly increased in TTL KO MEFs as compared to WT MEFs. In TTL KO MEFs, microtubule persistence dropped dramatically following MCAK overexpression and became similar to that observed in WT MEFs (Fig. 1C and Supplementary videos 3-4). MCAK depletion dramatically

increased microtubule persistence time, which overran the observation time in more than 80% of the cases, in both genotypes (Supplementary videos 5-6).

We compared microtubule dynamic instability in WT and TTL KO (Figure 1D and Supplementary Information, Figure S2). Microtubules in TTL KO MEFs displayed a higher frequency of rescues (3-fold), an increase of the time spent growing (2-fold) and a reduction of the time spent shrinking (2-fold). In TTL KO cells, MCAK overexpression resulted in a decrease in the frequency of rescues (2-fold) and a decrease in the time spent growing with a corresponding increase in the time spent pausing. MCAK depletion by siRNA increased the rescue frequency in WT cells (3-fold) and increased the time spent pausing at the expense of the time spent shrinking in both genotypes. Interestingly, the two genotypes no longer exhibited significant differences in microtubule dynamics in the presence of MCAK siRNA.

These results indicate a reduction of microtubule disassembly and abnormal microtubule persistence following membrane contact in TTL KO cells. MCAK overexpression partially rescued microtubule dynamic parameters in TTL KO MEFs and MCAK suppression erased the inherent differences between the genotypes. These data are compatible with a simple model where MCAK activity is impaired on detyrosinated microtubules. While no sizeable differences in MCAK expression were observed in TTL KO cells as compared to WT (Fig. S1 A-C), it is a formal possibility that MCAK activity could be affected indirectly.

To circumvent this, we assayed recombinant MCAK activity directly on the exposed microtubules of the two MEF genotypes, following cell lysis in a large volume of Triton based buffer to remove the cytosol. During lysis and further processing, microtubules were stabilized with 2 μM taxol to prevent spontaneous depolymerization. During the time course of experiments, in the absence of added exogenous MCAK, no detectable depolymerization of microtubules occurred, indicating negligible endogenous MCAK activity in lysed cell (not shown). WT MEFs contained tyrosinated microtubules and TTL KO MEFs exhibited

extensively detyrosinated microtubules and variable amounts of tyrosinated tubulin originating from tubulin synthesis (Peris et al., 2006) (Fig 2A). Fully detyrosinated microtubules could be generated by treating WT lysed fibroblasts with carboxypeptidase A (WT+CPA) (Fig. 2A). WT and WT + CPA lysed MEFs contained similar quantities of microtubule polymer (Fig. 2B-C). Lysed TTL KO fibroblasts also exhibited similar levels of microtubule polymer to that of WT fibroblasts (Fig. 2B-C). Following incubation with recombinant MCAK, WT microtubules displayed extensive depolymerization. In contrast, CPA treated WT microtubules or microtubules in TTL KO lysed fibroblasts were minimally affected by the addition of recombinant MCAK (Fig. 2B-C). Microtubule depolymerization was greater when TTL KO or WT + CPA microtubule arrays were incubated with a neck + motor domain mutant of MCAK instead of full length MCAK (Fig. 2C) but the extent of depolymerization was still less than that observed with WT microtubules (Fig. 2C). Microtubule exposure to the motor domain alone, which is devoid of sizeable depolymerizing activity (Maney et al., 2001), did not induce any detectable depolymerization of any microtubule array (Fig. 2C).

These results strongly indicate a direct relationship between microtubule detyrosination and MCAK inhibition which is evident even in the presence of the residual amounts of Tyr tubulin typically seen in TTL KO cells.

A possibility remained that tubulin detyrosination or CPA treatment inhibited MCAK by interfering with the interaction of the microtubules with other cellular effector proteins. To control for this possibility we assayed MCAK activity on microtubules assembled with purified tyrosinated or detyrosinated tubulin (Fig. 3A). MCAK activity on detyrosinated microtubules was diminished compared to tyrosinated microtubules, further supporting a direct relationship between microtubule tyrosination and MCAK activity (Fig. 3B-C). We then used microtubule binding assays to identify the point in the tubulin removal cycle that is

affected by tubulin tyrosination. MCAK's apparent affinity for microtubules is influenced by its nucleotide state (Helenius et al., 2006). Assays were run using the following nucleotides or nucleotide analogs: the non hydrolysable nucleotide analog AMP-PNP, which mimics the ATP collision state; ADP-ALFx, which mimics the ATP transition state ; ADP-vanadate, which mimics ADP-Pi ; and ADP (Fig. 4). By fluorescence microscopy, MCAK proteins yielded a punctuated decoration of microtubules, with some aggregates in the background (Fig. 4A), as previously observed (Moore and Wordeman, 2004). In quantitative studies, the AMP-PNP-bound forms of GFP-MCAK or of the GFP-neck + motor domain of MCAK associated to similar extents with tyrosinated or detyrosinated microtubules (Fig. 4B-C). In contrast, the ADP-AlFx-, ADP-vanadate- and ADP-bound forms of full length MCAK exhibited a diminished association with detyrosinated microtubules compared to tyrosinated polymers (Fig. 4B). The difference was maximal with the ADP-vanadate (Fig. 4B). Similar results were observed with the neck+motor domain of MCAK, although differences were smaller (Fig. 4C). Thus, detyrosination seems to diminish the affinity of the microtubule lattice for the ADP-Pi or ADP bound forms of MCAK.

To test whether the inhibition of depolymerizing motors was unique to TTL KO MEFs, we assayed TTL KO neurons for similar resistance to microtubule disassembly. When WT or TTL KO neurons were exposed to nocodazole, only residual tubulin staining was detectable in the axons of WT neurons whereas a persistent microtubule signal was evident in the axons of TTL deficient neurons (Fig 5A-C). Axonal microtubule disassembly is largely dependent on the activity of KIF2A (Homma et al., 2003), a neuronal kinesin-13 in the same family as MCAK. KIF2A KO neurons display morphogenetic anomalies affecting axonal length and branching (Homma et al., 2003). In an analysis of TTL KO neurons morphology we observed an increase in both the axon length and of the total length of axon collaterals. The number of primary collaterals per unit of axonal length was unaffected whereas the total number of

collaterals, including secondary or tertiary branches, was increased (Fig. 5D-G). These anomalies resemble those observed in KIF2A KO neurons (Homma et al., 2003). Collectively, our data strongly suggest that KIF2A activity is inhibited in TTL KO neurons and this is supported by experiments in lysed MEFs, showing inhibited KIF2A activity on WT CPA or TTL KO microtubules, compared to WT polymer (Fig. 5H).

The influence of the tubulin tyrosination status on the activity of depolymerizing motors provides an elegant mechanistic explanation for the observed stability of detyrosinated microtubules. Tubulin tyrosination affects the activity of the neck+motor mutant of MCAK which lacks both the N-terminal and the C-terminal domains of MCAK. This suggests that neither domain is centrally involved in MCAK interactions with the tubulin C-terminus. Both these domains are implicated in MCAK's ability to track on microtubule ends, which has been shown to be unaffected by tubulin detyrosination (Moore et al., 2005; Peris et al., 2006). Based on our data, microtubule detyrosination negatively affects MCAK's tubulin removal activity directly. Tubulin detyrosination, and its negative effect on kinesin-13 family motors, is thus the most likely explanation for the impairment of microtubule disassembly observed in TTL KO cells. A contribution of other modifications of the tubulin C-terminus, such as polyglutamylation, which could be affected by detyrosination and resulting microtubule stabilization, cannot be completely ruled out but polyglutamylation is minimal in cycling cells.

Our results suggest a direct role for tubulin detyrosination in MCAK inhibition and invalidate an indirect effect through CAP-Gly +TIP de-localization in TTL KO cells. Indeed, while microtubule detyrosination impairs CAP-Gly +TIP localization at + ends (Peris et al., 2006), this de-localization of CAP-Gly +TIP from microtubule ends induces a decrease in the rescue frequency and premature microtubule catastrophes close to membranes (Komarova et al.,

2002). In contrast, we observed the opposite microtubule dynamic parameters in TTL KO cells. Thus, we cannot attribute the increased microtubule stability to the absence of CAP-Gly +TIP at microtubule + ends.

The ADP-Pi- or ADP-bound forms of MCAK associate less efficiently with detyrosinated than with tyrosinated microtubules, suggesting that the lattice dwell time for MCAK between cycles of hydrolysis is lower on detyrosinated than on tyrosinated microtubules. This would substantially decrease the number of tubulin dimers removed per motor prior to detaching from the microtubule (Helenius et al., 2006; Wagenbach et al., 2008). It would also limit the ability of MCAK able to find microtubule ends by diffusive motility (Helenius et al., 2006).

In current models, the ADP-Pi or ADP forms of MCAK are retained in the vicinity of the microtubule lattice through weak electrostatic interaction with the charged E-hook of the α-tubulin C-terminus (Helenius et al., 2006). Our data demonstrate an important regulatory role for the C-terminal tyrosine of α-tubulin in the autoregulation of microtubule stability.

Impaired microtubule disassembly has been previously observed in KIF2A deficient neurons (Homma et al., 2003), or upon MCAK inhibition in cycling cells (Mennella et al., 2005). Obviously, kinesin-13 inhibition provides a highly plausible explanation for the impaired microtubule disassembly observed in different TTL KO cell types in this study. Additionally, MCAK appears to be important for microtubule disassembly upon encountering the cell edge, and may be crucial for end-on attachments to specific membrane complexes (Geiger et al., 1984; Morrison, 2007).

Impaired activity of depolymerizing motors may be central to several anomalies observed in TTL KO cells or mice. There is extensive overlap between the phenotypes observed in TTL KO or KIF2A KO neurons or mice (Erck et al., 2005; Homma et al., 2003). Anomalies and adaptations in depolymerizing motor activity may also be important for the facilitating effect of TTL loss on tumor progression (Mialhe et al., 2001). MCAK activity has been observed to

be altered in cancer cells (Hedrick et al., 2008; Ishikawa et al., 2008). Interestingly, both CAP-Gly + end binding proteins and depolymerizing motors have been identified as factors whose alteration favors genomic instability in aneuploid cells and thereby malignant cell invasiveness (Pellman, 2007; Storchova et al., 2006).

Factors able to promote the differentiation of cellular microtubules into distinct stability subclasses have been subject of sustained interest in cell biology. Decades ago, tubulin tyrosination, which distinguished with striking clarity between stable and dynamic microtubules, seemed to be an ideal mechanism responsible for selective microtubule stabilization (Schulze et al., 1987). This attractive view was discarded when it appeared that tyrosination *per se* does not alter microtubule dynamic properties. Based on our results, tubulin detyrosination could actually generate persistent stable microtubule subsets by rendering transiently stabilized microtubules resistant to motor-driven depolymerization.

MATERIALS AND METHODS

Antibodies: Detyr tubulin (L4), Tyr tubulin (clone YL1/2); α-tubulin (clone α3a) (Peris et al., 2006), polyclonal anti GFP (Invitrogen), polyclonal anti MCAK (Andrews et al., 2004).

Cell culture and transfection: Hippocampal neurons and MEFs (3 different embryos for each genotype) were prepared as in (Erck et al., 2005). MEF were transfected using AMAXA Biosystem and GFP–EB3 (N. Galjart, Rotterdam, The Netherlands); m-cherry α-tubulin (F. Saudou, Institut Curie, France) and m-cherry-MCAK (Wordeman's laboratory)**.** For inhibition of MCAK: Stealth siRNA Negative Control, Stealth Select siRNA #1 MSS232130; #2 MSS232131 and #3 MSS232132 from Invitrogen. MCAK inhibition was assayed by western blot analysis and siRNA #3 was used in microtubule dynamic analysis.

Recombinant proteins: The His_6-tagged HsKif2A neck + motor domain (residues 188 to 537) was expressed in BL21 bacterial strain. His_6-tagged- full length MCAK, $MCAK_{182-583}$ and EGFP-$MCAK_{182-583}$ were expressed in Baculovirus.

Nocodazole susceptibility assay: Cells were treated with carrier alone or with 20μM nocodazole for 60 min (neurons) or 15 min (MEFs), permeabilized in PHEM buffer (PIPES 60 mM, HEPES 25 mM, EGTA 10 mM, $MgCl_2$ 2 mM, pH 6,9) with 0.02% saponine and 10μM Taxol and fixed in PHEM buffer with 2% paraformaldehyde and 0.05 % glutaraldehyde. MT network was quantified by the α-tubulin fluorescence intensity measured inside the whole cell surface in fibroblasts (determined with F-actin staining) or in three fixed size regions (5 x 5 μm) placed at the proximal, medial and distal part of each axon.

Immunofluorescence and video-microscopy

Fluorescent images of living cells were captured with a charge-coupled device camera (CoolSNAP HQ; Roper Scienti c) using a 100/1.3 Plan-Neo fluar oil objective in an inverted motorized microscope (Axiovert 200M; Carl Zeiss MicroImaging, Inc.) controlled by MetaMorph software (Universal Imaging Corp.).

Fixed images were captured with a charge-coupled device camera(CoolSNAP ES; Roper Scientific) in a straight microscope (Axioskop 50;Carl Zeiss MicroImaging, Inc.) controlled by MetaView software (Universal Imaging Corp.) using a 40 or 100/1.3 Plan-Neo fluar oil objectives.

Analysis of MT behaviour: Image capture was every 3 seconds**.** MT displaying a trajectory at straight angle (70 to 110°) with the cell membrane were analysed inside a region of 10 µm from the cell edge. MT persistence time, measured for polymers whose growing end made contact with the membrane, was defined as the time during which at least a segment of MT kept running parallel to the membrane prior to disassembly. MT dynamic instability parameters were determined and analyzed as described in (Kline-Smith and Walczak, 2002).

Lysed cell experiments: Fibroblasts were lysed in PEM buffer (PIPES 80 mM, EGTA 1 mM, $MgCl_2$ 1 mM, pH 6,7) with 0.5% Triton X-100 and 10% glycerol and incubated PEM+2µM Taxol buffer in the presence or absence of 2 µg/ml Carboxypeptidase A (CPA, Sigma C-9268). Lysed cells were then washed in CPA inactivating buffer (20 mM DDT, PEM-Taxol buffer) and extensively washed in PEM-Taxol buffer. Lysed cells were incubated with buffer alone (PEM buffer, 2 µM taxol, 1 mM DTT, 75 mM KCl and 0.25 mM Mg-ATP) or with the same buffer containing purified motor protein (200 nM for MCAK proteins and 800 nM for KIF2A) for 30 minutes And then fixed in cold methanol. MT network was quantified by the α-tubulin fluorescence intensity measured inside the whole cell surface of lysed cells.

Motor binding to MTs was assayed in different nucleotide conditions: AMP-PNP; ADP-Aluminium Fluoride, ADP-Vanadate and ADP. Purified motors (1 µM) were incubated with nucleotides (2mM) and then with 0.01 µM Tyr or Detyr taxol-stabilized MTs (Paturle et al., 1989). Reactions were stopped with PEM, 50% Glycerol and 1% Glutaraldehyde and centrifuged on coverslips. MT-motor complexes were fixed in cold methanol and double stained with α-tubulin and GFP antibodies. For quantification, a line corresponding to each MT in the α-tubulin image was transferred to GFP images. The amount of motor bound per

unit of MT length was calculated as the percentage of positive GFP pixels versus total number of pixels in the MT line.

In vitro depolymerization experiments: taxol stabilized Tyr or Detyr MTs (10 nM) were incubated or not with MCAK-ATP (10 nM). Reactions were stopped with PEM, 50% Glycerol and 1% Glutaraldehyde after 10 or 20 min and centrifuged on coverslips. Reactions were fixed in cold methanol and stained with anti tubulin antibody. Quantification of total amount of MTs was measured using ImageJ software.

Data processing and analysis: Data were analyzed blind to the genotype or the experimental conditions. Statistical analysis: t-tests with unequal variances for samples comprising more than 30 measures or on parametric Mann and Whitney U test for smaller samples.

Online supplemental material

Fig S1 illustrates endogenous MCAK expression in WT or TTL KO MEFs and its specific suppression with commercial Stealth siRNAs. Fig S2 represents life history plots of individual microtubules from WT or TTL MEFs with endogenous levels, overexpression or suppression of MCAK. Videos 1 to 6 shows MT dynamics in a lamellipodia of a WT and TTL KO MEF respectively, with endogenous levels of MCAK (1-2), MCAK overexpression (3-4) and suppression (5-6).

ACKNOWLEDGEMENTS

We thank AA team's members for comments on the manuscript; D. Proietto, A. Schweitzer, JP. Andrieu and B. Dublet for technical help. This work was supported in part by grants: ANR Tyr-Tips to D.J., La Ligue contre le cancer to D.J.; ARC to D.J and A.A and NIH (GM069429) to LW.

Abbreviations: ADP·AlF_x, ADP+aluminium+sodium fluoride; AMP-PNP, p[NH]ppA, adenosine 5′-[β,γ-imido]triphosphate ; MEFs, mouse embryonic fibroblasts; MCAK, mitotic centromere-associated kinesin; MT, microtubule; KO, knock-out; TTL, tubulin tyrosine ligase.

Andrews, P.D., Y. Ovechkina, N. Morrice, M. Wagenbach, K. Duncan, L. Wordeman, and J.R. Swedlow. 2004. Aurora B regulates MCAK at the mitotic centromere. *Dev Cell*. 6:253-68.

Badin-Larcon, A.C., C. Boscheron, J.M. Soleilhac, M. Piel, C. Mann, E. Denarier, A. Fourest-Lieuvin, L. Lafanechere, M. Bornens, and D. Job. 2004. Suppression of nuclear oscillations in Saccharomyces cerevisiae expressing Glu tubulin. *Proc Natl Acad Sci U S A*. 101:5577-82.

Bieling, P., S. Kandels-Lewis, I.A. Telley, J. van Dijk, C. Janke, and T. Surrey. 2008. CLIP-170 tracks growing microtubule ends by dynamically recognizing composite EB1/tubulin-binding sites. *J Cell Biol*. 183:1223-33.

Erck, C., L. Peris, A. Andrieux, C. Meissirel, A.D. Gruber, M. Vernet, A. Schweitzer, Y. Saoudi, H. Pointu, C. Bosc, P.A. Salin, D. Job, and J. Wehland. 2005. A vital role of tubulin-tyrosine-ligase for neuronal organization. *Proc Natl Acad Sci U S A*.

Geiger, B., Z. Avnur, G. Rinnerthaler, H. Hinssen, and V.J. Small. 1984. Microfilament-organizing centers in areas of cell contact: cytoskeletal interactions during cell attachment and locomotion. *J Cell Biol*. 99:83s-91s.

Gupta, M.L., Jr., P. Carvalho, D.M. Roof, and D. Pellman. 2006. Plus end-specific depolymerase activity of Kip3, a kinesin-8 protein, explains its role in positioning the yeast mitotic spindle. *Nat Cell Biol*. 8:913-23.

Hammond, J.W., D. Cai, and K.J. Verhey. 2008. Tubulin modifications and their cellular functions. *Curr Opin Cell Biol*. 20:71-6.

Hedrick, D.G., J.R. Stout, and C.E. Walczak. 2008. Effects of anti-microtubule agents on microtubule organization in cells lacking the kinesin-13 MCAK. *Cell Cycle*. 7:2146-56.

Helenius, J., G. Brouhard, Y. Kalaidzidis, S. Diez, and J. Howard. 2006. The depolymerizing kinesin MCAK uses lattice diffusion to rapidly target microtubule ends. *Nature*. 441:115-9.

Homma, N., Y. Takei, Y. Tanaka, T. Nakata, S. Terada, M. Kikkawa, Y. Noda, and N. Hirokawa. 2003. Kinesin superfamily protein 2A (KIF2A) functions in suppression of collateral branch extension. *Cell*. 114:229-39.

Ishikawa, K., Y. Kamohara, F. Tanaka, N. Haraguchi, K. Mimori, H. Inoue, and M. Mori. 2008. Mitotic centromere-associated kinesin is a novel marker for prognosis and lymph node metastasis in colorectal cancer. *Br J Cancer*. 98:1824-9.

Khawaja, S., G.G. Gundersen, and J.C. Bulinski. 1988. Enhanced stability of microtubules enriched in detyrosinated tubulin is not a direct function of detyrosination level. *J Cell Biol*. 106:141-9.

Kline-Smith, S.L., and C.E. Walczak. 2002. The microtubule-destabilizing kinesin XKCM1 regulates microtubule dynamic instability in cells. *Mol Biol Cell*. 13:2718-31.

Komarova, Y.A., A.S. Akhmanova, S. Kojima, N. Galjart, and G.G. Borisy. 2002. Cytoplasmic linker proteins promote microtubule rescue in vivo. *J Cell Biol*. 159:589-99.

Maney, T., M. Wagenbach, and L. Wordeman. 2001. Molecular dissection of the microtubule depolymerizing activity of mitotic centromere-associated kinesin. *J Biol Chem*. 276:34753-8.

Manning, A.L., N.J. Ganem, S.F. Bakhoum, M. Wagenbach, L. Wordeman, and D.A. Compton. 2007. The kinesin-13 proteins Kif2a, Kif2b, and Kif2c/MCAK have distinct roles during mitosis in human cells. *Mol Biol Cell*. 18:2970-9.

Mennella, V., G.C. Rogers, S.L. Rogers, D.W. Buster, R.D. Vale, and D.J. Sharp. 2005. Functionally distinct kinesin-13 family members cooperate to regulate microtubule dynamics during interphase. *Nat Cell Biol*. 7:235-245.

Mialhe, A., L. Lafanechere, I. Treilleux, N. Peloux, C. Dumontet, A. Bremond, M.H. Panh, R. Payan, J. Wehland, R.L. Margolis, and D. Job. 2001. Tubulin detyrosination is a frequent occurrence in breast cancers of poor prognosis. *Cancer Res*. 61:5024-7.

Moore, A., and L. Wordeman. 2004. C-terminus of mitotic centromere-associated kinesin (MCAK) inhibits its lattice-stimulated ATPase activity. *Biochem J*. 383:227-35.

Moore, A.T., K.E. Rankin, G. von Dassow, L. Peris, M. Wagenbach, Y. Ovechkina, A. Andrieux, D. Job, and L. Wordeman. 2005. MCAK associates with the tips of polymerizing microtubules. *J Cell Biol*. 169:391-7.

Morrison, E.E. 2007. Action and interactions at microtubule ends. *Cell Mol Life Sci*. 64:307-17.

Newton, C.N., M. Wagenbach, Y. Ovechkina, L. Wordeman, and L. Wilson. 2004. MCAK, a Kin I kinesin, increases the catastrophe frequency of steady-state HeLa cell microtubules in an ATP-dependent manner in vitro. *FEBS Lett*. 572:80-4.

Ohi, R., K. Burbank, Q. Liu, and T.J. Mitchison. 2007. Nonredundant functions of Kinesin-13s during meiotic spindle assembly. *Curr Biol*. 17:953-9.

Paturle, L., J. Wehland, R.L. Margolis, and D. Job. 1989. Complete separation of tyrosinated, detyrosinated, and nontyrosinatable brain tubulin subpopulations using affinity chromatography. *Biochemistry*. 28:2698-704.

Pellman, D. 2007. Cell biology: aneuploidy and cancer. *Nature*. 446:38-9.

Peris, L., M. Thery, J. Faure, Y. Saoudi, L. Lafanechere, J.K. Chilton, P. Gordon-Weeks, N. Galjart, M. Bornens, L. Wordeman, J. Wehland, A. Andrieux, and D. Job. 2006. Tubulin tyrosination is a major factor affecting the recruitment of CAP-Gly proteins at microtubule plus ends. *J Cell Biol*. 174:839-49.

Saoudi, Y., I. Paintrand, L. Multigner, and D. Job. 1995. Stabilization and bundling of subtilisin-treated microtubules induced by microtubule associated proteins. *J Cell Sci*. 108 (Pt 1):357-67.

Schulze, E., D.J. Asai, J.C. Bulinski, and M. Kirschner. 1987. Posttranslational modification and microtubule stability. *J Cell Biol*. 105:2167-77.

Steinmetz, M.O., and A. Akhmanova. 2008. Capturing protein tails by CAP-Gly domains. *Trends Biochem Sci*.

Storchova, Z., A. Breneman, J. Cande, J. Dunn, K. Burbank, E. O'Toole, and D. Pellman. 2006. Genome-wide genetic analysis of polyploidy in yeast. *Nature*. 443:541-7.

Wagenbach, M., S. Domnitz, L. Wordeman, and J. Cooper. 2008. A kinesin-13 mutant catalytically depolymerizes microtubules in ADP. *J Cell Biol*. 183:617-23.

Webster, D.R., G.G. Gundersen, J.C. Bulinski, and G.G. Borisy. 1987. Assembly and turnover of detyrosinated tubulin in vivo. *J Cell Biol*. 105:265-76.

Figure 1. **Impaired MT dynamics in TTL KO MEFs.**

(A) Analysis of nocodazole effects on WT or TTL KO MEFs. Data is expressed as the ratio of MT signals measured after nocodazole treatment versus control conditions (mean ± s.e.m). MT signals were estimated for a minimum of 39 MEFs from 3 independent experiments, for each genotype and treatment conditions. *** $p<0.001$ *t* test (B) Video-microscopy examination of microtubules in WT or TTL KO MEFs expressing m-cherry α-tubulin and GFP-EB3, close to the leading edge of lamellipodial extensions. Color filled arrowheads: localization of the MT tip at different time points. Empty arrowheads of corresponding color: initial microtubule tip localization. Most WT MTs underwent extensive depolymerization following membrane contact (white and yellow arrowhead). Some MTs followed the leading edge for a short period of time prior to depolymerization (pink arrowhead). Most TTL KO MTs continued to grow after membrane touch, running along the plasma membrane or even growing inward (white arrowhead). Occasionally, MTs seemed to push the membrane forward prior to disassembly, rescue, and re-growth (yellow arrowhead). Similar phenotypes were observed when microtubule ends were labeled with other TIPs or in experiments run with fluorescent tubulin alone (not shown). Scale bar: 10 μm. (C) Measurement of the time spent by MTs exploring the area near the leading edge (persistence time). Experiments were run in control conditions or following cell transfection with either MCAK cDNA or MCAK siRNAs. At least 42 microtubules were examined in each condition. With MCAK siRNAs persistence times generally exceeded 100 seconds and overran the observation time (supplementary videos 5 and 6). Results are shown in other conditions as mean values ± s.e.m. *** $p<0.001$, *t* test. (D) Analysis of microtubule dynamic instability. Microtubules whose growing + tip was located within 10 μm of the leading edge at time zero were followed over time after various cell treatments, as indicated. Mean values ± s.e.m. Statistically

significant differences between WT and KO cells are described in the text, in all cases p values were <0.01 with Mann and Whitney U test.

Figure 2**. Depolymerizing activity of MCAK on tyrosinated or detyrosinated microtubules in lysed cells.**

(A) Microtubule tyrosination/detyrosination levels in lysed cells. WT or TTL KO MEFs were lysed in a triton based buffer, taxol-stabilized, fixed and labeled with tyrosinated and detyrosinated tubulin antibodies. WT+CPA: WT lysed MEFs incubated with CPA prior to fixation. Scale bar: 50 µm. (B) MCAK effects on lysed cells. Images of MT arrays in control conditions or following exposure to recombinant full length MCAK. Scale bar: 50 µm. (C) Quantitative analysis of MT depolymerization in the presence of full length MCAK or MCAK domains. MT signal: percentage ± s.e.m. of the area occupied by the MT network versus total cell area. A minimum of 78 lysed cells were analyzed in each condition. *** p<0.001, *t* test.

Figure 3**. Depolymerizing activity of MCAK on pure tyrosinated or detyrosinated microtubules.**

(A) Tyrosinated and detyrosinated microtubules stained for either total, tyrosinated or detyrosinated tubulin. (B) Representative pictures of tyrosinated and detyrosinated MT before and after exposure to MCAK for 20 min. Scale bar: 10 µm (C) Analysis of MT depolymerization in the presence MCAK. MT signal: percentage ± s.e.m. of the area occupied by MT at time 10 or 20 min versus time 0. A minimum of 20 independent images were measured in each condition. ** p<0.01 *** p<0.001, *t* test.

Figure 4**. Tubulin tyrosination affects the interaction of MCAK with microtubules.**

(A) Fluorescence images of MCAK binding to microtubules. Taxol-stabilized, tyrosinated or detyrosinated pure tubulin MTs (10 nM, red) were incubated with 0.25 µM purified GFP-MCAK (green) in AMP-PNP or ADP-Va bound forms. Scale bar: 5 µm. (B-C) Quantitative analysis of full length MCAK (B) or MCAK neck + motor domain (C) association with 10 nM of pure Tyr or Glu MTs at different motor concentration and in the presence of various nucleotides. Motor binding was measured as the ratio of the motor signal versus MT signal (MCAK per MT %). Mean ± s.e.m. At least 100 MTs were analyzed for each condition.

Figure 5**. Impaired MT disassembly and abnormal cell morphology in TTL KO cultured neurons.**

(A-B) WT or TTL KO hippocampal neurons 2 days after plating. Neurons were incubated in the absence (Control, A) or presence of 20 µM Nocodazole (B), permeabilized in saponin based buffer to extract free tubulin molecules, and double labeled for F-actin (red) and tubulin (green). Scale bar: 20 µm. (C) Quantitative analysis of nocodazole effects. The axonal microtubule signal was expressed as the ratio of MT signals measured after nocodazole treatment versus control conditions (mean values ± s.e.m). Microtubule signals were estimated for a minimum of 50 axons from 3 independent experiments. (D-G) Cell morphology in WT or TTL KO neurons, showing length, number of primary or of higher order collaterals and total length of collaterals. Mean values ± s.e.m. for 93 WT neurons and 123 TTL KO neurons from 3 independent experiments. (H) Depolymerizing activity of neck+motor construct of KIF2A on tyrosinated or detyrosinated microtubules. Assay was as in figure 2C. Mean values ± s.e.m for 75 cells. *** $p<0.001$, *t* test.

Figure S1: Endogenous MCAK distribution and expression levels in WT and TTL KO fibroblasts.

A Immunofluorescence images of fibroblasts labelled with alpha-tubulin (red) and MCAK (green) antibodies. MCAK is enriched in lamellipodial extensions in both WT and TTL KO cells. However, MCAK seems to colocalize with MT network (insert) in WT cells extensions, whereas it shows a more diffuse pattern in TTL KO cells extensions (insert), compatible with a diminished lateral association of MCAK with microtubules. Note that MCAK comets, which are unaffected by tubulin detyrosination, (Peris et al. 2006) are not detected with MCAK antibody. Scale bar: 50 µm.

B Quantitative analysis of MCAK versus MTs signals at the leading edge and in the perinuclear region of cells. Ratio of MCAK versus α-tubulin fluorescent signals in a fixed size region located near the leading edge or close to the nucleus. Data are expressed as mean values + s.e.m. for 74 WT fibroblasts and 70 TTL KO fibroblasts from three independent experiments (*** $p<0.001$ using parametric t test). The ratio MCAK/α-tubulin in lamellipodial extensions was lower in TTL KO cells compared to WT cells.

C Western blot analysis of MCAK content in WT or TTL KO fibroblast extracts. Equal amounts of proteins were loaded in each lane.

D Western blot analysis of MCAK levels in WT or TTL KO fibroblast transfected with Stealth siRNA Negative Control or with 3 different commercial MCAK siRNAs from Invitrogen (#1: MSS232130, #2: MSS232131 and #3: MSS232132). Equal amounts of proteins were loaded in each lane. Since MCAK depletion is almost complete 36 h after transfection of siRNA #3, such conditions have been used in all MCAK depletion experiments.

Figure S2: Analysis of microtubule dynamic instability

Representative life history plots of individual microtubules, in various conditions as indicated. The corresponding statistical analysis is shown Figure 1D.

A-B Microtubule rescues are more frequent in TTL KO cells compared to WT. As a result, microtubule catastrophes leading to extensive depolymerization are a more frequent occurrence in WT cells than in TTL KO cells.

C-D MCAK over-expression leads to more precocious large microtubule catastrophes in WT cells. In TTL KO cells, MCAK over expression reduces the number of rescues and increases the time spent pausing by polymers at the expense of the time spent growing.

E-F MCAK depletion with siRNAs induces an attenuation of microtubule dynamic instability behaviour in both genotypes, with a decrease in the time spent shrinking and an increase in the time spent pausing. As a result of MCAK depletion, microtubule dynamic instability behaviour becomes similar in both genotypes.

Supplementary methods

Endogenous MCAK distribution and levels in WT or TTL KO fibroblasts.

WT or TTL KO fibroblasts were fixed with 4% paraformaldehyde and 4% Sucrose in PBS buffer. Fixed cells were double stained with α-tubulin and MCAK antibodies. To quantify the MCAK enrichment in lamellipodial extensions, two fixed size regions (5 x 5 µm) were located near the leading edge or close to the nucleus. Fluorescence intensities were measured for α-tubulin and MCAK labeling and a ratio of MCAK versus α-tubulin fluorescent signals was calculated. To analyse MCAK content in aWT or TTL KO fibroblast extract, cells were cultured for 48 h in DMEM/10% FBS, washed in warm PBS and scrapped in laemli sample buffer. Equal amounts of proteins were loaded and analyzed by SDS-PAGE gel.

MCAK depletion in WT or TTL KO fibroblasts.

WT and TTL KO fibroblasts were transfected using AMAXA Biosystem with 3 µg of Stealth siRNA Negative Control or with 3 different MCAK siRNAs (Stealth Select siRNA 1 to 3; as described in methods). Cells were cultured for 24 and 36 h in DMEM/10% FBS, washed in warm PBS and scrapped in laemli sample buffer. Equal amounts of proteins were loaded and analyzed by SDS-PAGE gel.

Supplementary Video 1
Time-lapse video-microscopy of a lamellipodial extension of a WT fibroblast expressing mcherry α-tubulin (red) and GFP-EB3 (green). Representative MTs are marked with arrowheads. When MTs reach the cell edge, MT tips stop growing and often undergo a complete depolymerization until disappearance from the peripheral area (effective catastrophe; white and yellow arrowhead). Only a small proportion of MTs follow the leading edge for a while before depolymerizing (pink arrowhead).

Images from the red and green channels were taken every 3 seconds, for 3 minutes. Time is expressed in min:s. Scale bar: 10 μm.

Supplementary Video 2
Time-lapse video-microscopy of a lamellipodial extension of a TTL KO fibroblast expressing m-cherry α-tubulin (red) and GFP-EB3 (green). Representative MTs are marked with arrowheads. MT tips in TTL KO cells do not pause upon reaching the membrane but instead, continue to grow. As a result, as they approach the membrane, they turn away from the cell edge or sometimes they run along the plasma membrane (white arrowhead). Occasionally, when some MTs contact the leading edge, they seem to push the membrane forward for a while (yellow arrowhead). This phenotype has also been observed in KIF2A KO cells.

Images from the red and green channels were taken every 3 seconds, for 3 minutes. Time is expressed in min:s. Scale bar: 10 μm.

Supplementary Video 3
Time-lapse video-microscopy of a lamellipodial extension of a WT fibroblast expressing mcherry MCAK (red) and GFP-EB3 (green). Representative MTs are marked with arrowheads. MT behaviour is perturbed with MCAK overexpression leading to a complete depolymerization until disappearance from the lamellipodial extension after membrane contact.

Images from the red and green channels were taken every 3 seconds, for 3 minutes. Time is expressed in min:s. Scale bar: 10 μm.

Supplementary Video 4
Time-lapse video-microscopy of a lamellipodial extension of a TTL KO fibroblast expressing m-cherry MCAK (red) and GFP-EB3 (green). Representative MTs are marked with arrowheads. MT behaviour is perturbed with MCAK overexpression in TTL KO cells. Some MTs undergo catastrophes after contact with the cell membrane (light blue arrow), some spend time pausing (red arrow) and only a small proportion follows the leading edge and never shrinks (white arrow).

Images from the red and green channels were taken every 3 seconds, for 3 minutes. Time is expressed in min:s. Scale bar: 10 μm.

Supplementary Video 5
Time-lapse video-microscopy of a lamellipodial extension of a WT fibroblast treated with MCAK siRNA for 36 h and expressing m-cherry α-tubulin (red) and GFP-EB3 (green). Representative MTs are marked with arrowheads. MCAK depletion induced an attenuation of microtubule dynamics in WT cells. When MTs reach the cell edge, they turn away and grow continuously; alternating phases of growing and pausing (white and light blue arrows).

Images from the red and green channels were taken every 3 seconds, for 3 minutes. Time is expressed in min:s. Scale bar: 10 μm.

Supplementary Video 6
Time-lapse video-microscopy of a lamellipodial extension of a TTL KO fibroblast treated with MCAK siRNA for 36 h and expressing m-cherry α-tubulin (red) and GFP-EB3 (green). Representative MTs are marked with arrowheads. MCAK depletion induced an attenuation of microtubule dynamics in TTL KO cells. When MTs reach the cell edge, they turn away and continue polymerizing, alternating phases of growing and pausing (white and red arrows) as observed in WT siRNA treated cells.

Images from the red and green channels were taken every 3 seconds, for 3 minutes. Time is expressed in min:s. Scale bar: 10 μm.

Figure 1- L. Peris

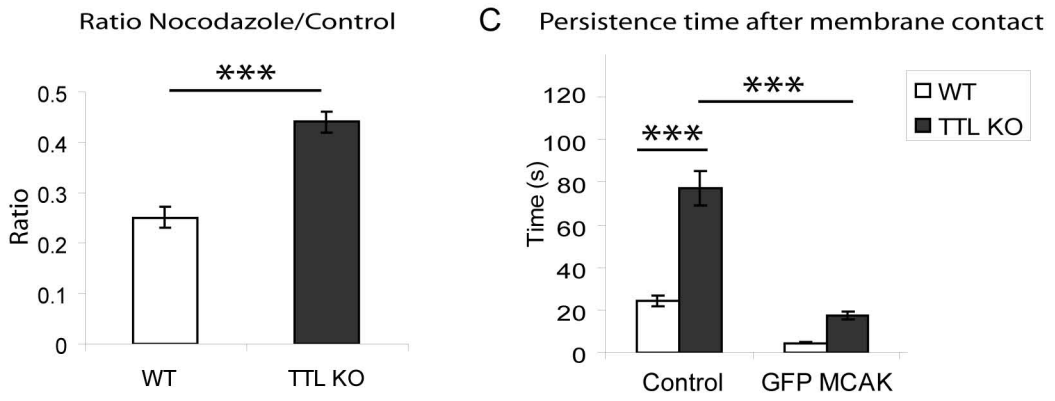

B

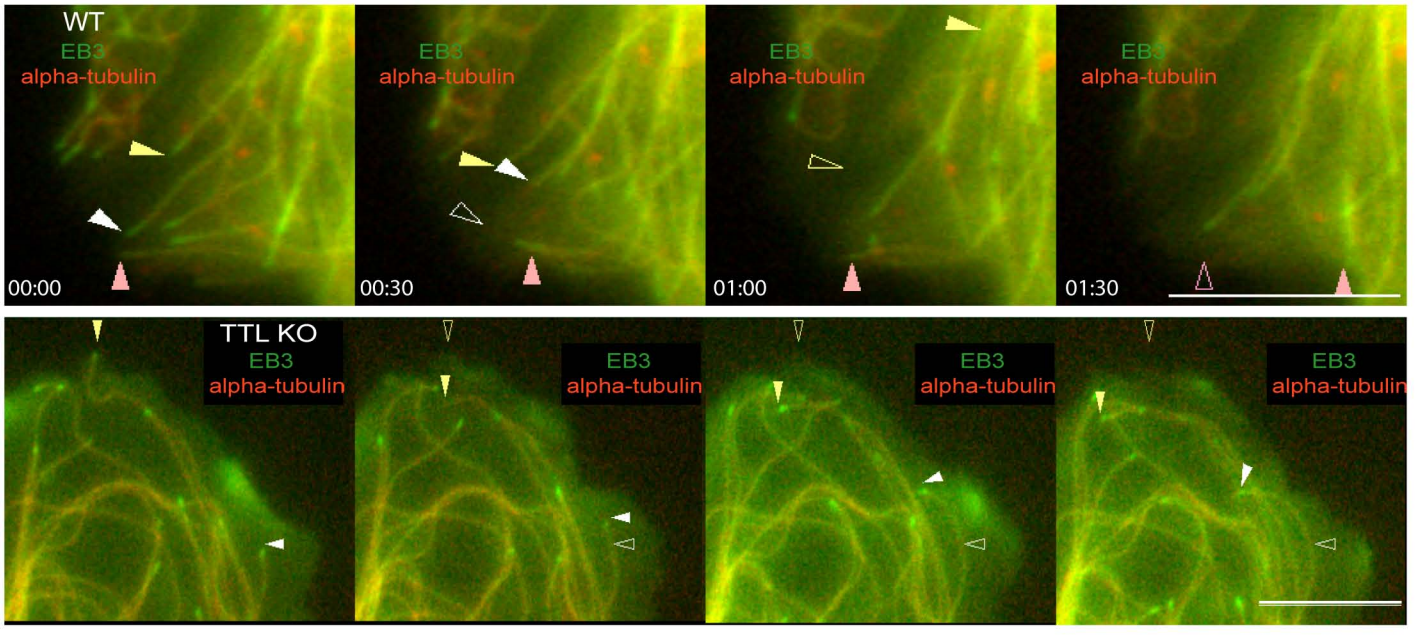

D

	Control		+ MCAK		si RNA MCAK	
	WT	TTL-null	WT	TTL-null	WT	TTL-null
Catastrophe frequency (min-1) (± s. e. m)	1.47 ± 0.22	0.99 ± 0.17	2.25 ± 0.34	1.21 ± 0.19	0.97 ± 0.18	0.60 ± 0.10
Rescue frequency (min-1) (± s. e. m)	0.75 ± 0.23	2.30 ± 0.41	1.29 ± 0.31	1.34 ± 0.23	2.37 ± 0.37	2.06 ± 0.22
Growth rate (µm/min) (± s. e. m)	12.07 ± 1.48	12.58 ± 1.38	12.25 ± 1.15	10.77 ± 1.06	14.50 ± 1.52	16.72 ± 0.92
Shrinking rate (µm/min) (± s. e. m)	20.61 ± 1.69	23.66 ± 2.40	17.98 ± 1.45	17.65 ± 1.36	22.40 ± 1.65	24.32 ± 2.15
% Time growing (± s. e. m)	35.27 ± 2.83	54.89 ± 4.80	27.89 ± 4.92	25.45 ± 3.27	36.01 ± 3.43	33.48 ± 2.79
% Time shrinking (± s. e. m)	27.22 ± 1.93	12.69 ± 1.93	33.00 ± 3.93	14.83 ± 2.52	8.38 ± 1.35	7.41 ± 1.43
% Time pausing (± s. e. m)	30.02 ± 3.25	27.47 ± 5.22	32.44 ± 6.28	56.69 ± 4.12	48.61 ± 4.66	48.77 ± 4.17
% MT never shrinking	0.00	10.00	0.00	4.55	15.79	0.00
% MT never growing	0.00	0.00	19.05	4.55	0.00	5.00
Number of MT analyzed	n = 21	n = 20	n = 21	n = 22	n = 19	n = 20
Number of cells analyzed	n = 4	n = 4	n = 4	n = 6	n = 5	n = 5

Figure 2- L. Peris

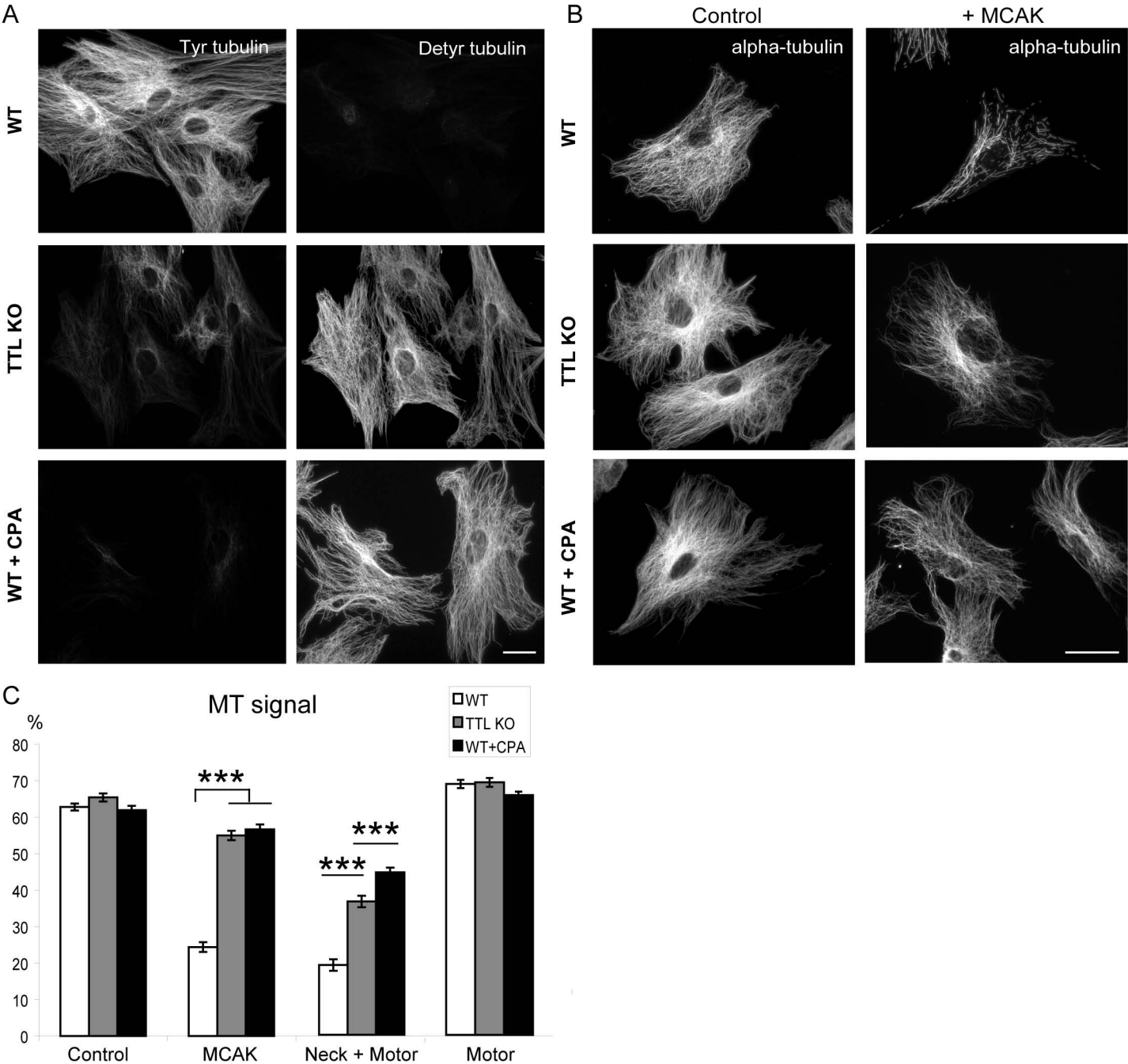

Figure 3- L. Peris

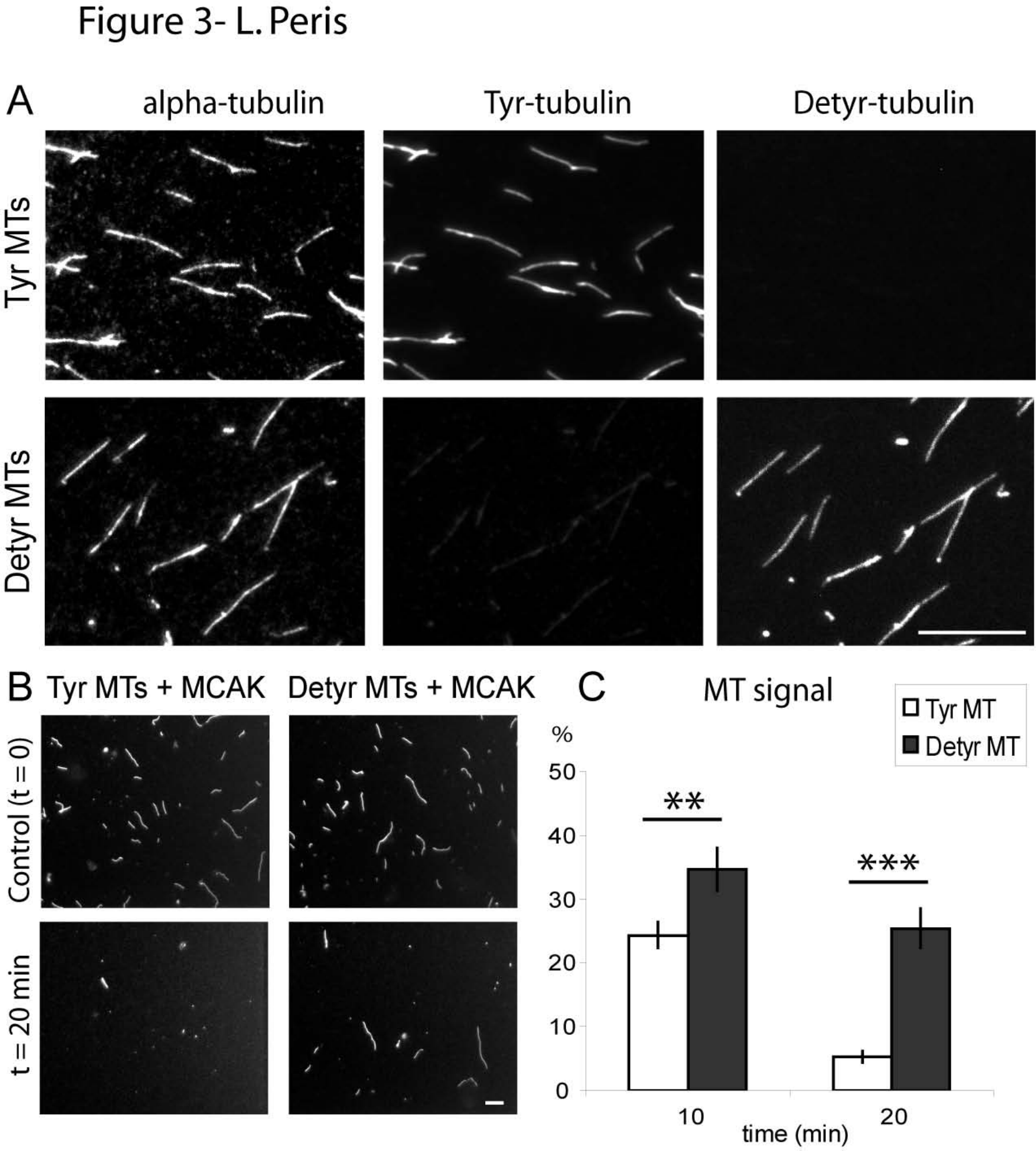

Figure 4- L. Peris

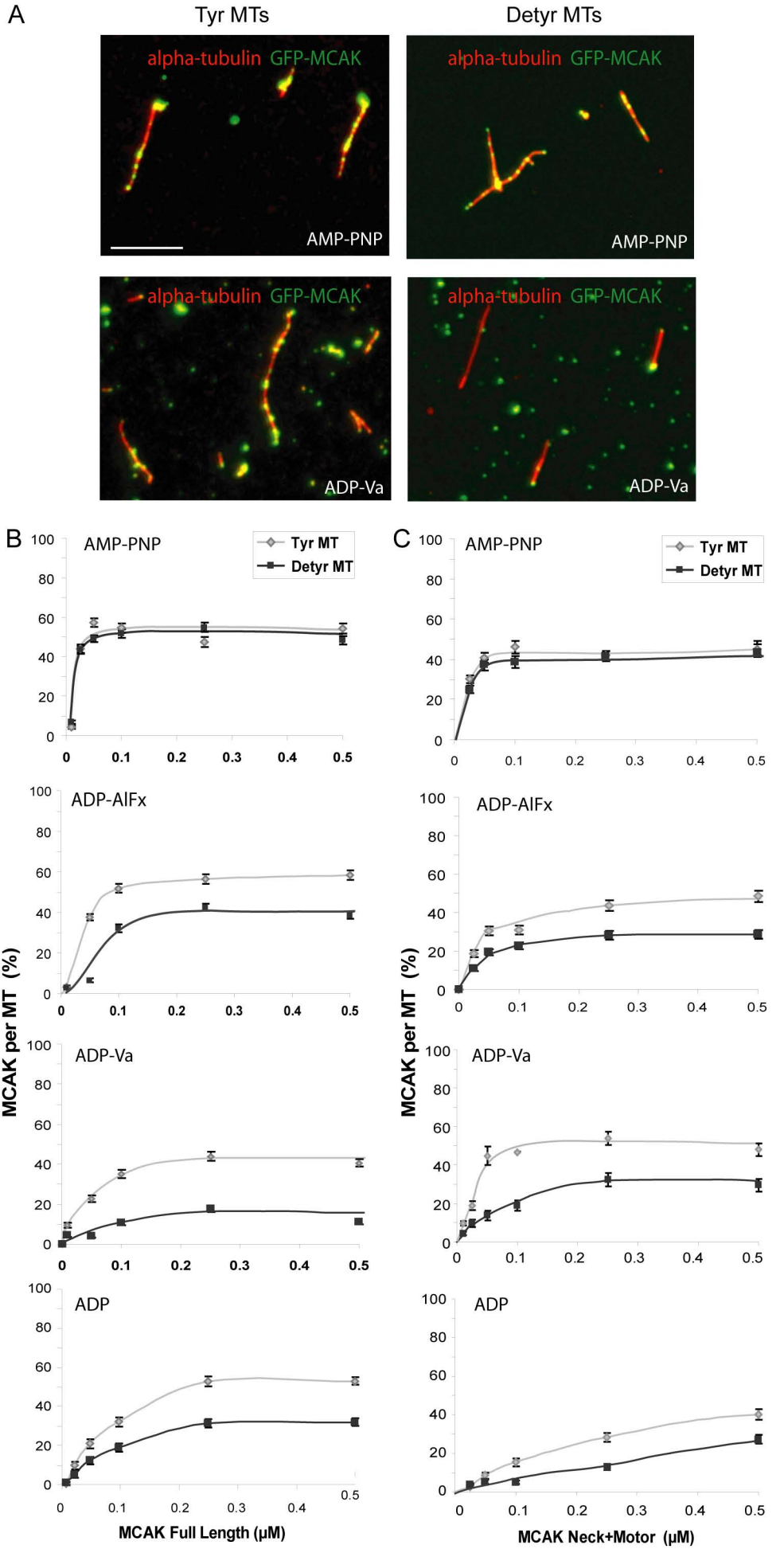

Figure 5 - L. Peris

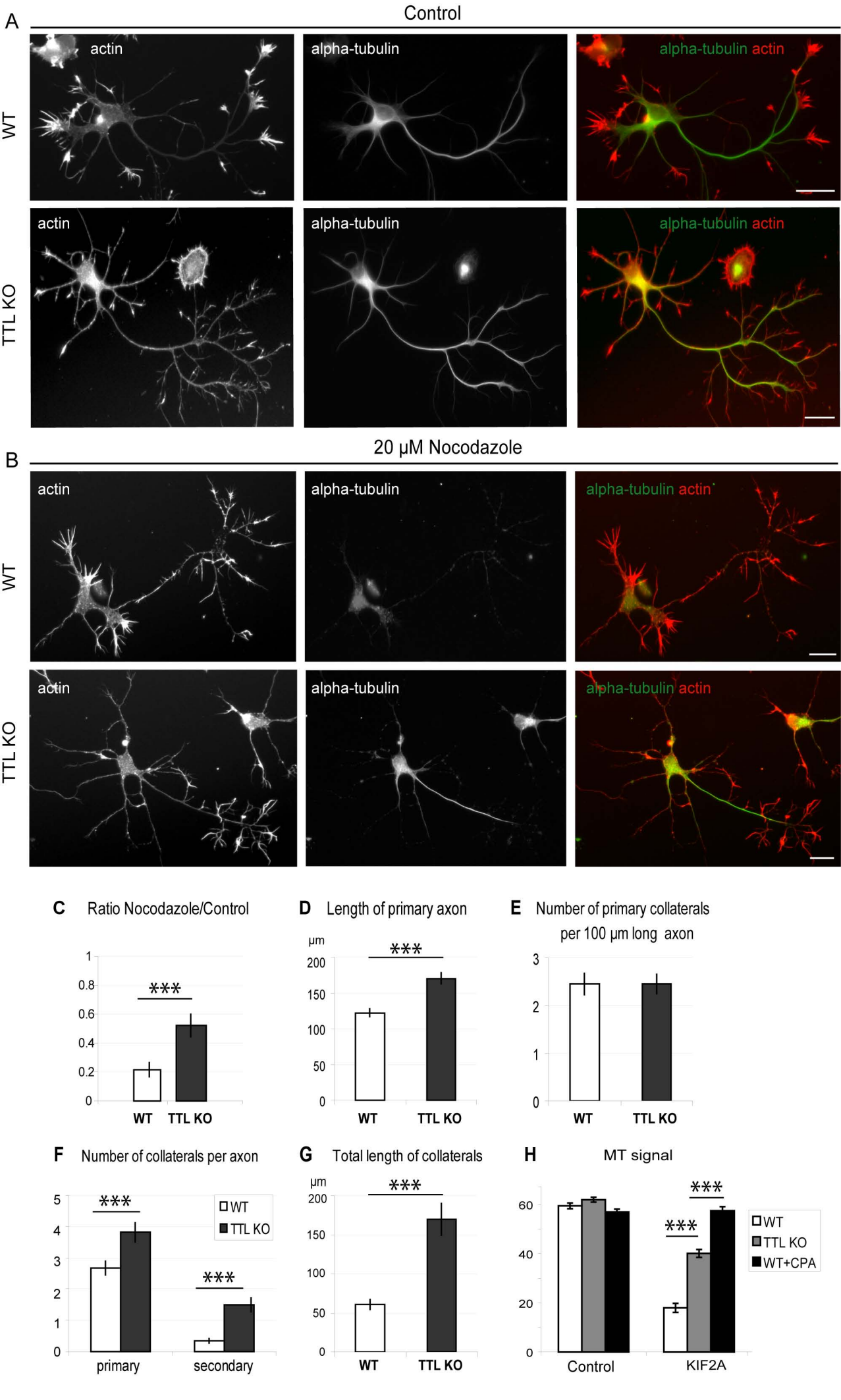

Supplementary figure S1- L. Peris

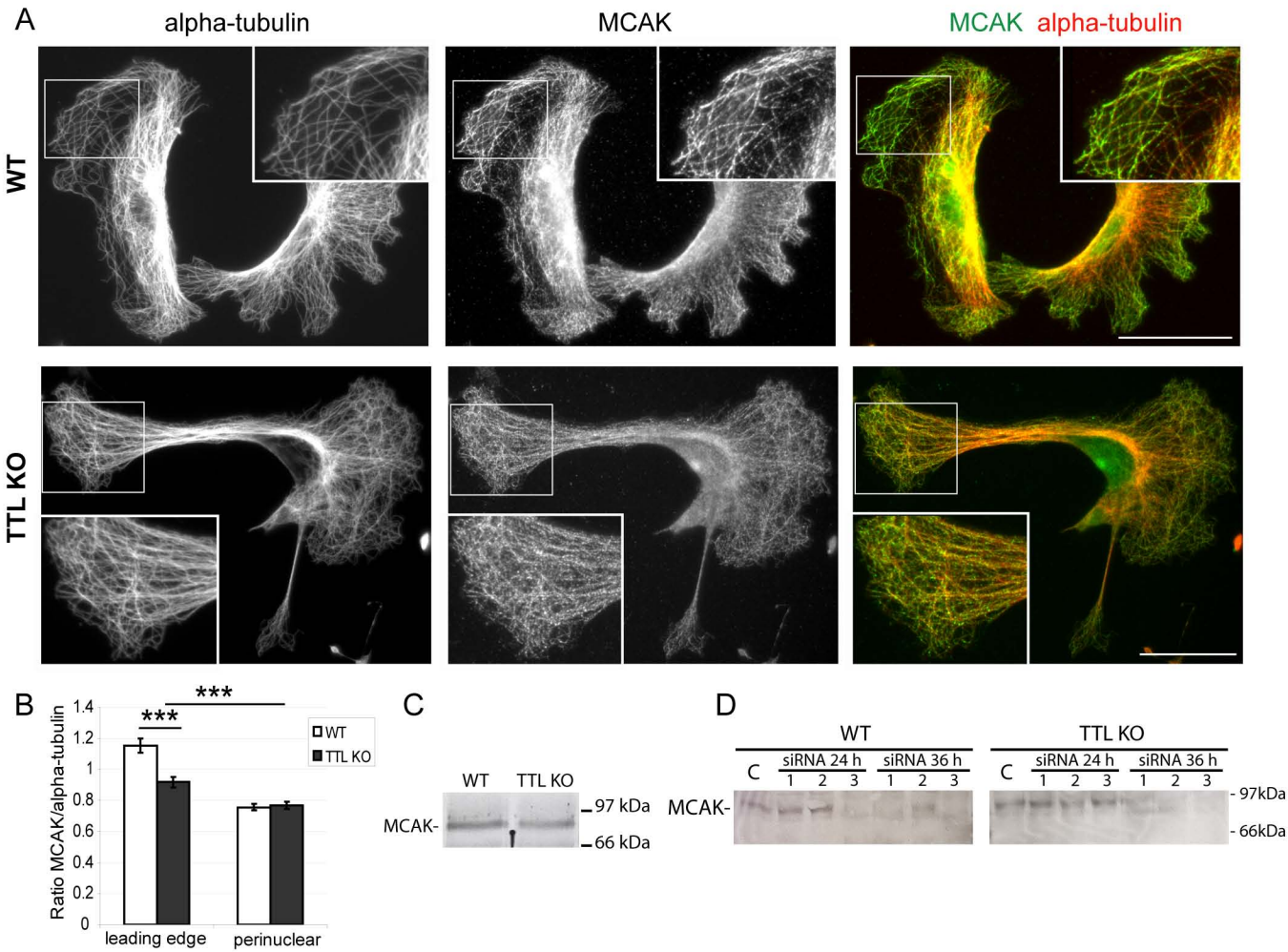

Figure S1: Endogenous MCAK distribution and expression levels in WT and TTL KO fibroblasts.
(A) Immunofluorescence images of fibroblasts labelled with α-tubulin (red) and MCAK (green) antibodies. MCAK is enriched in lamellipodial extensions in both WT and TTL KO cells. However MCAK seems to colocalize with MT network (insert) in WT cells extensions, whereas it shows a more diffuse pattern in TTL KO cells extensions (insert), compatible with a diminished lateral association of MCAK with microtubules. Note that MCAK comets, which are unaffected by tubulin detyrosination, (Peris et al. 2006) are not detected with MCAK antibody. Scale bar: 50 µm.
(B) Quantitative analysis of MCAK versus MTs signals at the leading edge and in the perinuclear region of cells. Ratio of MCAK versus α-tubulin fluorescent signals in a fixed size region (5 x 5 µm) located near the leading edge or close to the nucleus. Data are expressed as mean values + s.e.m. for 74 WT fibroblasts and 70 TTL KO fibroblasts from three independent experiments (*** $p<0.001$ using parametric t test). The ratio MCAK/α-tubulin in lamellipodial extensions was lower in TTL KO cells compared to WT cells.
(C) Western blot analysis of MCAK content in WT or TTL KO fibroblast extracts. Equal amounts of proteins were loaded in each lane.
(D) Western blot analysis of MCAK levels in WT or TTL KO fibroblast transfected with Stealth siRNA Negative Control or with 3 different commercial MCAK siRNAs from Invitrogen (#1: MSS232130, #2: MSS232131 and #3:

Supplementary figure S2- L. Peris

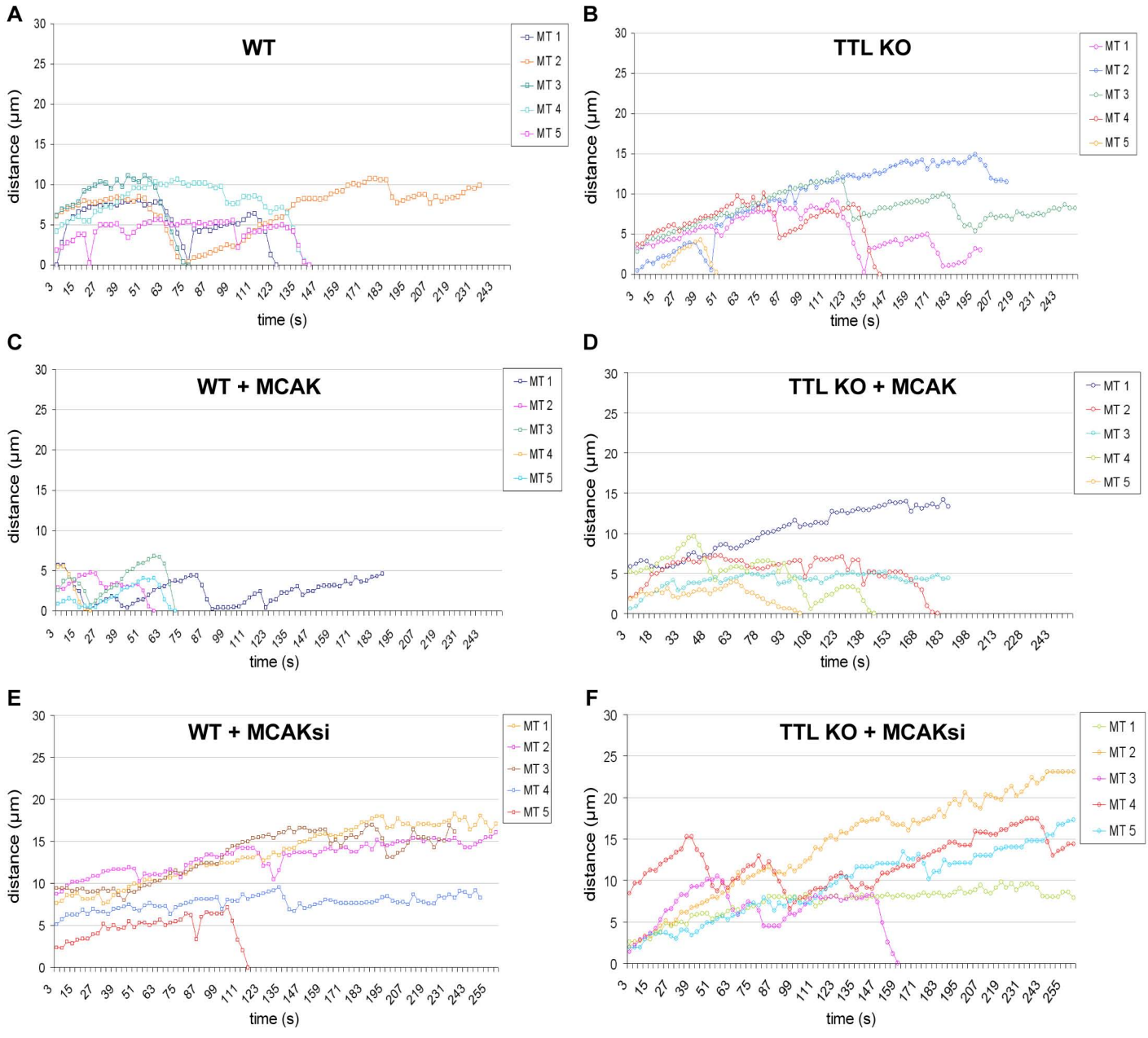

Figure S2: Analysis of microtubule dynamic instability

Representative life history plots of individual microtubules, in various conditions as indicated. The corresponding statistical analysis is shown Figure 1D.

(A-B) Microtubule rescues are more frequent in TTL KO cells compared to WT. As a result, microtubule catastrophes leading to extensive depolymerization are a more frequent occurrence in WT cells than in TTL KO cells.

(C-D) MCAK over-expression leads to more precocious large microtubule catastrophes in WT cells. In TTL KO cells, MCAK over expression reduces the number of rescues and increases the time spent pausing by polymers at the expense of the time spent growing.

(E-F) MCAK depletion with siRNAs induces an attenuation of microtubule dynamic instability behaviour in both genotypes, with a decrease in the time spent shrinking and an increase in the time spent pausing. As a result of MCAK depletion, microtubule dynamic instability behaviour becomes similar in both genotypes.